Journal of Catalysis **205,** 289–293 (2002)
doi:10.1006/jcat.2001.3458, available online at http://www.idealibrary.com on IDEAL®

Carbon Deposition and Catalytic Deactivation during CO_2 Reforming of CH_4 over Co/γ-Al_2O_3 Catalysts

E. Ruckenstein[1] and H. Y. Wang

Department of Chemical Engineering, State University of New York at Buffalo, Amherst, New York 14260

Received May 31, 2001; revised October 22, 2001; accepted October 22, 2001; published online January 3, 2002

The reaction behavior and carbon deposition during the CO_2/CH_4 reforming reaction have been investigated over the γ-Al_2O_3-supported Co catalysts as a function of Co loading (between 2 and 20 wt%) and calcination temperature ($T_c = 500$ or 1000°C). It was found that the stability of Co/γ-Al_2O_3 catalysts was strongly dependent on the Co loading and calcination temperature. For some loadings (6 wt% for $T_c = 500$°C and 9 wt% for $T_c = 1000$°C), stable activities have been achieved. However, over the catalysts with high Co loadings (>12 wt%), notable amounts of carbon were accumulated during reforming, and deactivation was observed. Moreover, severe deactivation was also noted over the 2 wt% catalysts, both when carbon deposition occurred ($T_c = 500$°C) or was absent ($T_c = 1000$°C). In the latter case, the oxidation of the metallic sites was responsible for the deactivation. Hence, there are two different deactivation mechanisms, namely, carbon deposition and oxidation of metallic sites. The activities were stable when a balance between carbon formation and its oxidation could be achieved. © 2002 Elsevier Science

Key Words: **carbon dioxide reforming of methane; synthesis gas; Co catalyst; deactivation.**

1. INTRODUCTION

The catalytic CO_2 reforming of CH_4 (reaction 1), in which a mixture of CH_4 and CO_2, both greenhouse gases, is converted to synthesis gas, has been comprehensively studied for the past few years (1–35). The synthesis gas thus generated has a low H_2/CO ratio (≤ 1) and is therefore suitable for the Fischer–Tropsch synthesis of higher hydrocarbons and for the oxo-synthesis or synthesis of oxygenates (36, 37).

$$CH_4 + CO_2 \rightarrow 2CO + 2H_2, \quad \Delta H^0_{298} = 247 \text{ kJ/mol} \qquad [1]$$

Most of the group VIII metals are more or less catalytically active toward this reaction. Due to the inherent inertness of methane, a high temperature (typically, 800–900°C) is needed to achieve a meaningful yield. Under such severe conditions, an excess carbon deposition occurs on the surface of the catalyst, and this constitutes a major drawback. Even though the noble metal-based catalysts (such as Rh, Ru, Pd, and Pt) can provide high activity and selectivity with little or no carbon deposition (2, 5), they are unsuitable for large-scale commercial use because of their limited availability. While Ni- and Co-based catalysts are easily available, they deactivated rapidly when the conventional supports, such as Al_2O_3 and SiO_2, were employed. Exceptions were the cases in which MgO was used as support (10, 16, 34, 35). There is general agreement that the catalytic deactivation during the CO_2 reforming of methane is caused by carbon deposition and/or sintering of the metal particles (2, 3, 5, 12, 17, 24, 28, 32). Sintering accelerates the carbon deposition since large metal ensembles stimulate coke formation (38).

Numerous mechanistic studies have suggested that during the CH_4/CO_2 reforming, CH_4 is decomposed on the metallic sites to reactive carbon species (CH_x, $x = 0$–3), which are oxidized to CO by the oxygen-containing species that originate from CO_2 (2, 4, 5, 8, 13, 18, 21, 30). Consequently, the rate of carbon accumulation on the catalyst surface is determined by the relative rates of the generation of carbon species and its oxidative removal. When the former is faster than the latter, excess carbon deposition will occur. The goal of the present paper was to correlate the carbon deposition with the catalytic deactivation. For this purpose, the CO_2 reforming of CH_4 was investigated over γ-Al_2O_3-supported Co catalysts as a function of Co loading and calcination temperature (T_c) and the amount of carbon deposits generated during the reforming reaction was determined. It was found that besides the carbon deposition, the oxidation of the metallic sites by CO_2 also caused deactivation. Conditions could be identified under which the activity of the catalyst remained stable as a result of a dynamic balance between carbon formation and its oxidation.

2. EXPERIMENTAL

2.1. *Catalyst Preparation*

The supported cobalt catalysts were prepared by impregnating γ-Al_2O_3 with aqueous solutions of $Co(NO_3)_2 \cdot 6H_2O$, followed by overnight drying at 110°C and calcination in the open air of a furnace at 500 or 1000°C for

---

[1] To whom correspondence should be addressed. Fax: (+1-716) 6453822.

0021-9517/02 $35.00

TABLE 1

Physical Data for the γ-Al_2O_3-Supported Co Catalysts

Co loading (Wt%)	T_c (°C)	BET surf. area[a] (m^2/g-cat.)	Co surf. area[b] (m^2/g-cat.) (×100)
2	500	77	48
	1000	51	15
6	500	77	83
	1000	44	26
9	500	78	91
	1000	46	34
12	500	71	109
	1000	40	39
20	500	66	154
	1000	35	49

[a] For the calcined catalysts.

[b] For the reduced catalysts.

8 h. The calcined catalysts are denoted as Co(O)/γ-Al_2O_3 (500 or 1000°C). The catalysts reduced in H_2 are denoted as Co/γ-Al_2O_3 (500 or 1000°C). The temperatures inside the parentheses refer to the calcination temperature (T_c). Co loading means weight percent Co in the completely reduced catalyst.

2.2. *Catalytic Reaction*

The catalytic assay was carried out under atmospheric pressure in a fixed-bed vertical quartz reactor (i.d. 4 mm), which was operated in a down-flow mode. The calcined catalyst (20.0 mg) was held on a quartz wool bed and its reduction was carried out in a H_2 flow (30 ml/min) by increasing the temperature from room temperature to 600°C at a rate of 20°C/min and from 600 to 900°C at a rate of 10°C/min, without holding at 900°C. After reduction, the feed gases ($CH_4/CO_2 = 1/1$) were introduced into the catalyst bed at a flow rate of 20 ml/min, which for 20.0 mg of catalyst corresponds to a space velocity of 6.0×10^4 ml h^{-1} g^{-1}. The reactants and products were analyzed with an online gas chromatograph (GC) equipped with a Porapak Q column. An ice-cold trap was set between the reactor exit and the GC sampling valve to remove the water formed during reaction.

2.3. *Catalyst Characterization*

2.3.1. BET surface area and the exposed Co surface area. The BET surface area of the calcined catalysts and the exposed Co surface area of the reduced catalysts, determined as in our previous paper (34), are listed in Table 1.

2.3.2. Coke determination. The amount of carbon deposited on the catalyst surface during the CO_2/CH_4 reforming reaction was determined by oxidizing the carbon to CO with CO_2 in a pulse reactor. A quartz tube (i.d. 4 mm), in which the used catalyst was held on a quartz wool bed, was employed as reactor. The used catalyst was heated to 900°C in a flow of He (35 ml/min) to remove the possible adsorbed species (such as water and CO_2) and then pulses of CO_2 (500 μl) were injected into the carrier gas (He, 35 ml/min). The reaction product, CO, was analyzed with an online gas chromatograph equipped with a thermal conductivity detector (TCD) and a Porapak Q column. Through the CO_2 oxidation of the reduced catalysts, it was found that the CO that resulted via the oxidation of the metallic sites was, with the exception of the 2 and 6 wt% catalysts precalcined at 1000°C, much smaller than those that resulted from the deposited carbon. For the exceptions, the amount of carbon deposited was negligibly small.

2.3.3. X-ray photoelectron spectroscopy (XPS). Samples were mounted on double-sided adhesive tapes and the XPS data were obtained with a SSI Small Spot ESCA system using monochromatized Al$K\alpha$ radiation ($h\nu = 1.485$ keV). The pressure in the ion-pumped analysis chamber was below 2×10^{-9} Torr during data acquisition. The binding energies were referenced to the adventitious C 1s line (284.8 eV).

3. RESULTS AND DISCUSSION

As reported previously (39), in the γ-Al_2O_3-supported Co catalysts, the species generated during calcination were strongly dependent on the calcination temperature (T_c): Co_3O_4 was generated as a major phase at a T_c of 500°C, and Co_2AlO_4 and $CoAl_2O_4$ were generated at a T_c of 1000°C. As shown in Table 1, for the same Co loading, Co/γ-Al_2O_3 (500°C) had after reduction a larger exposed Co surface area than did Co/γ-Al_2O_3 (1000°C) because of the higher reducibility of Co_3O_4. For this reason, their catalytic performances in the CO_2/CH_4 reforming were expected to be different. The time-dependent activities of the Co/γ-Al_2O_3 (500°C) and Co/γ-Al_2O_3 (1000°C) catalysts are plotted in Figs. 1 and 2. Only the conversion of

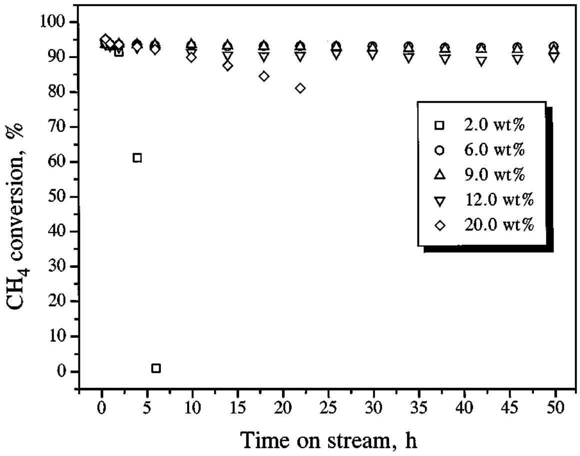

FIG. 1. Time-dependent conversion of CH_4 over the reduced Co/γ-Al_2O_3 (500°C) catalysts. $P = 1$ atm, $T = 900$°C, $CH_4/CO_2 = 1.0$, space velocity = 60 000 ml h^{-1} g^{-1}.

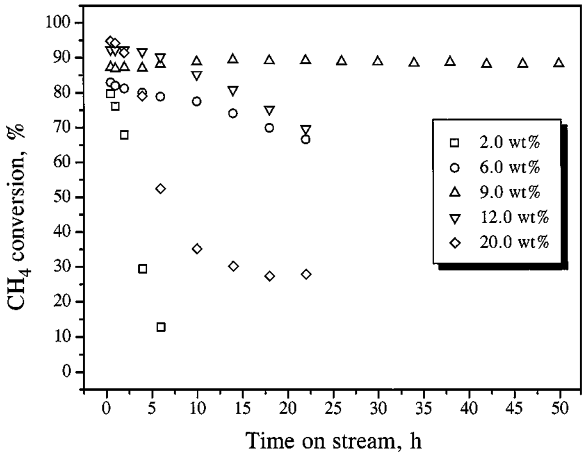

FIG. 2. Time-dependent conversion of CH_4 over the reduced Co/γ-Al_2O_3 (1000°C) catalysts. $P = 1$ atm, $T = 900°C$, $CH_4/CO_2 = 1.0$, space velocity $= 60\,000$ ml h^{-1} g^{-1}.

CH_4 is presented, because the conversion of CO_2 and the yields to H_2 and CO follow the same pattern. The equilibrium conversion of CH_4 at a reaction temperature of 900°C is about 96.8. As shown in Figs. 1 and 2, in most cases the initial activities of Co/γ-Al_2O_3 catalysts are close to the equilibrium value. With time on stream, some catalysts deactivated, while others maintained their initial activities. At a T_c of 500°C, severe deactivation occurred over the catalysts with low (2 wt%) and high (20 wt%) loadings, while no significant deactivation was observed during 50 h over those with loadings between 6 and 12 wt% (Fig. 1). At a T_c of 1000°C, the 9 wt% catalyst provided a stable activity during 50 h, while all the others experienced deactivation to various extents (Fig. 2). Figures 1 and 2 demonstrate that the stability of Co/γ-Al_2O_3 catalysts in the CO_2/CH_4 reforming reaction was strongly affected by the Co loading and the calcination temperature.

TABLE 2

Coke Deposition and Catalytic Deactivation during CO_2/CH_4 Reforming over the Reduced Co/γ-Al_2O_3 Catalysts

Co loading (wt%)	T_c (°C)	Reaction time (h)	Amount of coke (mol) ($\times 10^6$)	Deactivation[a] (%)
2	500	6	101.2	99.0
	1000	6	0.2	83.9
6	500	22	13.2	0.8
		50	31.1	1.1
	1000	22	0.3	19.6
9	500	22	132.5	0.8
		50	189.3	2.1
	1000	22	114.3	−2.2
12	500	6	162.4	0.4
		22	258.1	3.6
		50	308.5	4.0
	1000	22	711.6	24.5
20	500	6	420.3	3.2
		22	733.9	14.7
	1000	22	1447.5	70.6

[a] Defined as the difference between the initial (after 0.5 h) and final CH_4 conversions with respect to the initial one and multiplied by 100.

The amount of carbon accumulated on the catalyst surface during reaction is listed in Table 2. To correlate the carbon deposition with the catalytic deactivation, the deactivation, which is defined as the difference between the initial (after 0.5 h) and final CH_4 conversions with respect to the initial one, is also included in Table 2. Figures 3a and 3b plot the amount of carbon deposited and the deactivation as a function of Co loading for a selected reaction time. At a T_c of 500°C, both exhibited a minimum at a loading of 6 wt% (Fig. 3a), indicating that the carbon deposition, which decreases the number of exposed metallic sites, was one cause for catalytic deactivation. At a T_c of 1000°C and for Co loadings higher than 9 wt%, both increase with increasing Co loading (Fig. 3b), indicating again that the carbon

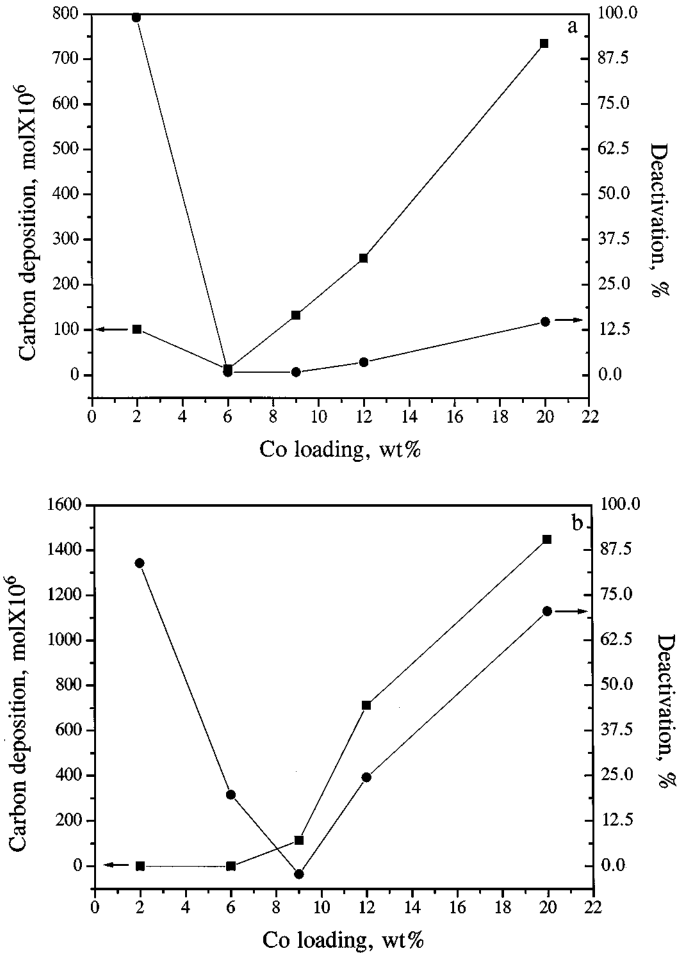

FIG. 3. Carbon deposition and deactivation as a function of Co loading over the Co/γ-Al_2O_3 (500°C) (a) and Co/γ-Al_2O_3 (1000°C) (b). (The data employed are after 22 h of reaction, with the exception of the 2 wt% catalyst which after 6 h had small CH_4 conversions.)

TABLE 3

Color of the γ-Al_2O_3-Supported Catalysts after Various Treatments

Co loading (wt%)	T_c (°C)	After calcination	After reduction	After reforming reaction
2	500	Light green	Dark gray	Black
	1000	Light blue	Gray	Light blue
6	500	Black	Black	Black
	1000	Blue	Blue-gray	Blue (surface layer) Blue-gray (the rest)
9	500	Black	Black	Black
	1000	Blue	Blue-gray	Black
12	500	Black	Black	Black
	1000	Dark blue	Black	Black
20	500	Black	Black	Black
	1000	Dark blue	Black	Black

deposition was responsible for deactivation. However, for Co loadings lower than 9 wt%, severe deactivation occurred even though almost no carbon deposition could be detected (Fig. 3b). This implies that besides carbon deposition there is also another cause for catalytic deactivation. The color changes observed under various conditions provided some useful information. As shown in Table 3, the 2 wt% Co/γ-Al_2O_3 (1000°C) catalyst had after the reforming reaction the same light blue color as after calcination. The 6 wt% Co/γ-Al_2O_3 (1000°C) catalyst had after the reforming reaction a thin blue top layer, as after calcination, while the rest was blue-gray, as after reduction. Since after calcination at $T_c = 1000$°C, Co_2AlO_4 and $CoAl_2O_4$ were generated in the Co(O)/γ-Al_2O_3 catalysts, these color changes indicate that a large number of metallic Co sites were oxidized and restructuring of catalysts took place (to form Co_2AlO_4 and $CoAl_2O_4$) during the reforming reaction over the Co/γ-Al_2O_3 (1000°C) catalysts with Co loadings below 9 wt%. Consequently, the oxidation of the metallic sites, which decreases the total number of metallic sites, constitutes another cause for catalytic deactivation.

For the Co/γ-Al_2O_3 (500°C) catalysts, it should be noted that while the carbon deposition was much lower over the 2 wt% catalyst than over the 20 wt% one, the deactivation was much higher over the former than over the latter. To provide a reasonable explanation, the reactivity of carbon generated during the reforming reaction toward CO_2 was examined in a pulse reactor (i.d. 4 mm) at 900°C by pulsing CO_2 over the used 2, 6, 12, and 20 wt% Co/γ-Al_2O_3 (500°C) catalysts, which had been subjected for 6 h to the reforming reaction. The amount of CO formed as a function of the CO_2 pulse number is plotted in Fig. 4. For the first pulse point, the amount of CO formed was much lower over the 2 and 6 wt% catalysts than over the 12 and 20 wt% ones. Over the 2 wt% catalyst, the amount of CO formed decreased moderately during the first five pulses, and very slowly during the following 45 pulses, while over the 6 wt% catalyst, it decreased to practically zero after 12 pulses. Except for the 2 wt% catalyst, the amount of CO generated for the last pulse point was negligible compared to the total amount of CO formed. Figure 4 demonstrates that the carbon deposited on the 2 wt% catalyst was more difficult to remove with CO_2 than were those deposited over the 6, 12, and 20 wt% catalysts. This could have been caused either by the lower reactivity of the carbon deposited over the 2 wt% catalyst or by the smaller number of active sites present in this catalyst or, possibly, by both. As demonstrated by XPS (Fig. 5), the peaks of C 1s of the used 2 and 20 wt% catalysts were centered at 285.0 eV, which could be assigned to a −C−C− type deposit (26). Thus, the carbons deposited on the 2 and 20 wt% catalysts had the same

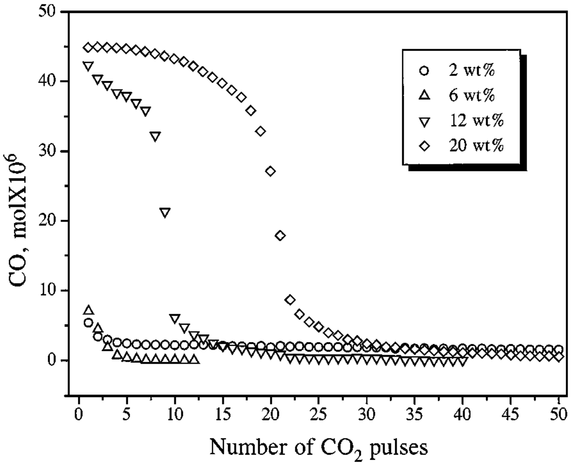

FIG. 4. Amount of CO formed as a function of CO_2 pulse number during the reaction between surface carbon and CO_2 over the Co/γ-Al_2O_3 (500°C) catalysts that were exposed to the reforming reaction for 6 h under the following conditions: $P = 1$ atm, $T = 900$°C, $CH_4/CO_2 = 1.0$, space velocity = 60 000 ml h^{-1} g^{-1}.

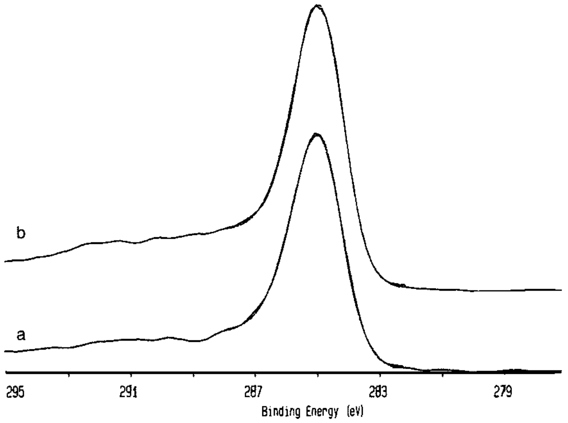

FIG. 5. C 1s XPS spectrum obtained over the 2 (a) and 20 (b) wt% Co/γ-Al_2O_3 (500°C) catalysts that were exposed to the reforming reaction for 6 h under the following conditions: $P = 1$ atm, $T = 900$°C, $CH_4/CO_2 = 1.0$, space velocity = 60 000 ml h^{-1} g^{-1}.

nature. Consequently, the difficulty in the removal of the carbon deposited on the 2 wt% catalyst with CO_2 was due to the fewer accessible metallic Co sites available; most of them were covered by carbon. This explains why after 6 h of reaction the 2 wt% catalyst almost lost its activity for the CO_2 reforming of methane (Fig. 1) and also demonstrates that metallic Co sites are required for the reaction between the surface carbon and CO_2.

In the literature, two mechanisms have been suggested for the CO_2/CH_4 reforming. Mark and Maier (7, 15) suggested an Eley–Rideal mechanism for the CO_2 reforming, in which methane is adsorbed and decomposed over the metal (Rh) into H_2 and adsorbed carbon, and the carbon reacts directly with CO_2 from the gas phase generating CO. In an alternative mechanism (2, 4, 5, 8, 13, 18, 21, 30), methane is decomposed on the metal to yield a surface CH_x species and adsorbed hydrogen. On sorption, CO_2 dissociates to CO and adsorbed oxygen, and the oxygen reacts with the CH_x species to generate CO and hydrogen. Our results are compatible with the second mechanism because of the oxidation of the metallic sites by CO_2.

In summary, due to the coexistence of reductive (CH_4, H_2, and CO) and oxidative (CO_2 and H_2O) species in CO_2/CH_4 reforming, the atmosphere in the reactor is both reductive and oxidative. During reaction, a fraction of Co^0 is oxidized to Co–O, which is reduced again to Co^0 by carbon species, thereby generating a dynamic redox process. The reductive atmosphere stimulates the regeneration of metallic Co and the dissociative adsorption of CH_4, while the oxidative atmosphere favors the oxidation of metallic Co sites. When the former dominates (as over the 20 wt% catalysts), an excess of carbon is deposited; when the latter dominates (as over the 2 wt% Co/γ-Al_2O_3 (1000°C) catalyst), the number of metallic sites is decreased due to their oxidation and subsequent restructuring of catalysts. Both lead to severe catalytic deactivations. Consequently, the catalysts are stable when there is a balance between the generation of carbon species and its oxidative removal. By optimizing the metal loading (6 wt% for $T_c = 500^\circ$C and 9 wt% for $T_c = 1000^\circ$C), highly effective and stable Co/γ-Al_2O_3 catalysts can be obtained.

REFERENCES

1. Gadalla, A. M., and Bower, B., *Chem. Eng. Sci.* **43**(11), 3049 (1988).
2. Richardson, J. T., and Paripatyadar, S. A., *Appl. Catal.* **61**, 293 (1990).
3. Ashcroft, A. T., Cheetham, A. K., Green, M. L. H., and Vernon, P. D. F., *Nature* **352**, 225 (1991).
4. Solymosi, F., Kutsan, Gy., and Erdöhelyi, A., *Catal. Lett.* **11**, 149 (1991).
5. Rostrup-Nielsen, J. R., and Hansen, J-H. B., *J. Catal.* **144**, 38 (1993).
6. Erdöhelyi A., Cserényi J., and Solymosi, F., *J. Catal.* **141**, 287 (1993).
7. Mark, M. F., and Maier, W. F., *Angew. Chim. Int. Ed. Engl.* **33**(15/16), 1657 (1994).
8. Qin, D., and Lapszewicz, J., *Catal. Today* **21**, 551 (1994).
9. Nakamura, J., Aikawa, K., Sato, K., and Uchijima, T., *Catal. Lett.* **25**, 265 (1994).
10. Ruckenstein, E., and Hu, Y. H., *Appl. Catal. A* **133**, 149 (1995).
11. Zhang, Z. L., and Verykios, X. E., *J. Chem. Soc. Chem. Commun.* 71 (1995).
12. Zhang, Z. L., Tsipouriari, V. A., Efstathiou, A. M., and Verykios, X. E., *J. Catal.* **158**, 51 (1996).
13. Qin, D., Lapszewicz, J., and Jiang, X., *J. Catal.* **159**, 140 (1996).
14. Kroll, V. C. H., Swaan, H. M., and Mirodatos, C., *J. Catal.* **161**, 409 (1996).
15. Mark, M. F., and Maier, W. F., *J. Catal.* **164**, 122 (1996).
16. Hu, Y. H., and Ruckenstein, E., *Catal. Lett.* **36**, 145 (1996).
17. Zhang, Z. L., Verykios, X. E., MacDonald, S. M., and Affrossman, S., *J. Phys. Chem.* **100**, 744 (1996).
18. Hu, Y. H., and Ruckenstein, E., *Catal. Lett.* **57**, 167 (1999).
19. Bhat, R. N., and Sachtler, W. M. H., *Appl. Catal. A* **150**, 279 (1997).
20. Ruckenstein, E., and Hu, Y. H., *Appl. Catal. A* **154**, 185 (1997).
21. Wang, H. Y., and Au, C. T., *Appl. Catal. A* **155**, 239 (1997).
22. Chen, Y. G., Tomishige, K., Yokoyama, K., and Fujimoto, K., *Appl. Catal. A* **165**, 335 (1997).
23. Bitter, J. H., Seshan, K., and Lercher, J. A., *J. Catal.* **176**, 93 (1998).
24. Stagg, S. M., Romeo, E., Padro, C., and Resasco, D. E., *J. Catal.* **178**, 137 (1998).
25. Lemonidou, A. A., Goula, M. A., and Vasalos, I. A., *Catal. Today* **46**, 175 (1998).
26. Wang, S., and Lu, G. Q., *Appl. Catal. A* **169**, 271 (1998).
27. Tomishige, K., Chen, Y., and Fujimoto, K., *J. Catal.* **181**, 91 (1999).
28. Bitter, J. H., Seshan, K., and Lercher, J. A., *J. Catal.* **183**, 336 (1999).
29. Chen, Y. G., Tomishige, K., Yokoyama, K., and Fujimoto, K., *J. Catal.* **184**, 479 (1999).
30. Matsui, N., Anzai, K., Akamatsu, N., Nakagawa, K., Ikenaga, N., and Suzuki, T., *Appl. Catal. A* **179**, 247 (1999).
31. Wei, J. M., Xu, B. Q., Li, J. L., Cheng, Z. X., and Zhu, Q. M., *Appl. Catal. A* **196**, L167 (2000).
32. Kim, J. H., Sub, D. J., Park, T. J., Kim, and K. L., *Appl. Catal. A* **197**, 191 (2000).
33. Wang, H. Y., and Ruckenstein, E., *Appl. Catal. A* **204**, 143 (2000).
34. Ruckenstein, E., and Wang, H. Y., *Appl. Catal. A* **204**, 257 (2000).
35. Wang, H. Y., and Ruckenstein, E., *Appl. Catal. A* **209**, 207 (2001).
36. Trimm, D. L., *Catal. Rev.–Sci. Eng.* **16**, 155 (1977).
37. Xu, B. Q., and Sachtler, W. M. H., *J. Catal.* **180**, 198 (1998).
38. Rostrup-Nielsen, J. R., *in* "Catalysis Science and Technology" (J. R. Anderson and M. Boudart, Eds.), Vol. 5, pp. 1–118. Springer-Verlag, Berlin, 1984.
39. Wang, H. Y., and Ruckenstein, E., *Catal. Lett.* **75**, 13 (2001).